CELLULAR RESPONSE TO ORDERED COLLAGEN LAYERS ON MICA

A Thesis

by

WEE WEN LEOW

Submitted to the Office of Graduate Studies of
Texas A&M University
in partial fulfillment of the requirements for the degree of

MASTER OF SCIENCE

May 2012

Major Subject: Biomedical Engineering

CELLULAR RESPONSE TO ORDERED COLLAGEN LAYERS ON MICA

A Thesis

by

WEE WEN LEOW

Submitted to the Office of Graduate Studies of
Texas A&M University
in partial fulfillment of the requirements for the degree of

MASTER OF SCIENCE

Approved by:

Chair of Committee,	Wonmuk Hwang
Committee Members,	Roland R. Kaunas
	Andreea Trache
Head of Department,	Gerard L. Cote

May 2012

Major Subject: Biomedical Engineering

ABSTRACT

Cellular Response to Ordered Collagen Layers on Mica. (May 2012)
Wee Wen Leow, B.S., Texas A&M University
Chair of Advisory Committee: Dr. Wonmuk Hwang

Extracellular microenvironment, including its components and biophysical parameters such as matrix structure and stiffness, is a crucial determinant of cellular function. There exists an interdependency between cellular behaviors and the extracellular matrix (ECM), whereby cells are constantly sensing and modifying their surroundings in response to physical stress or during processes like wound repair, cancer cell invasion, and morphogenesis, to create an environment which supports adaptation. To date, knowledge of the distint regulatory mechanisms of this complex relationship is little, while the urge is evident as it plays a significant role in understanding tissue remodeling. Cells are observed to align with the parallel arrays of collagen fibrils found in tissues such as bone, tendon, and cornea, suggesting the importance of ordered matrices in defining cell functions. In this study, epitaxial growth of ordered two-dimensional collagen matrices were created, with parallelly aligned fibrils on muscovite mica, and novel triangular pattern matrix on phlogopite mica. Using Fluorescence and Atomic Force Microscopy, we were able to observe cell polarization along with stress fiber formation and matrix deformation at high resolution. Cells were observed to be able to penetrate between collagen fibrils and generate traction anisotropically to polarize. These ordered collagen matrices serve as an excellent model to study cellular remodeling of ECM in vitro, in which this fundamental apprehension of cell-matrix relationship is of crucial importance to manipulate the system and obtain desired cell functions.

ACKNOWLEDGMENTS

I would like to thank my research advisor, Dr. Wonmuk Hwang, for his patience, guidance and support over the course of my undergraduate and graduate programs. I would also like to thank my committee members, Dr. R. Kaunas and Dr. A. Trache, for their helpful insights and advices throughout the research.

Besides, I would like to extend my appreciation to several graduate students who helped me throughout the research. Abhishek Tandon and Hui-Ju Hsu taught me various procedures on cell cultures. I thank Dr. A. Yeh, Po-feng Lee, and Yu-qiang Bai for the generous gift of mTG samples.

I thank my current and previous lab members, Dr. John Noel, Dr. Sirish Kaushik Lakkaraju, Dr. Krishnakumar Mayuram Ravikumar, Xiaojing Teng, Andrew Liao, Amol Patel, and Esma Eryilmaz for their input at various junctures of this project.

Finally, I also thank my friends here at College Station for supporting me throughout this project.

TABLE OF CONTENTS

CHAPTER Page

I INTRODUCTION 1

A. Ordered two-dimensional collagen layers 2
B. Cell adhesion via mechanotransduction 3
C. Cellular remodeling of ECM 4

II MATERIALS AND METHODS 6

A. Preparation of ordered 2-D collagen layers 6
B. Cell culture 8
C. Cell seeding and fixing 8
D. AFM imaging 8

III RESULTS 10

A. Formation of 2D collagen layers 10
1. Assembly of unidirectionally aligned collagen layers on muscovite mica 10
2. Formation of triangular collagen networks on phlogopite mica 11
3. Layers morphology depends on potassium concentration 12
4. Addition of glycine and cross-linking with mTG 13
B. Cell-matrix interactions 14
1. Anisotropic cellular remodeling of collagen layers on muscovite 14
2. Cells on triangular collagen networks on phlogopite . . 15

IV DISCUSSION 16

A. Formation of 2D collagen layers 16
B. 2D collagen layers as a model to study cell-matrix interactions 18

V SUMMARY AND CONCLUSION 21

REFERENCES 22

APPENDIX A 30

CHAPTER Page

VITA 40

LIST OF FIGURES

FIGURE		Page
1	Schematic view of the integrin at (A) inactive, (B) active and (C) homo-oligomerization state.	30
2	AFM images of SAOS cell seeded on 2D aligned collagen layers.	31
3	Overview of the materials and methods.	32
4	Early stages of collagen assembly on muscovite.	33
5	AFM topography of triangular collagen networks on phlogopite, comparing the effects of glycine.	34
6	Effect of K^+ on collagen assembly.	35
7	AFM topography of aligned collagen fibrils on muscovite mica, comparing the effects of glycine.	36
8	AFM topography of collagens and cells on muscovite mica after 20 hours of cell seeding.	36
9	Fluorescence image of U2OS cells on non-cross-linked aligned collagens on muscovite, taken 22.5 hours after cell seeding.	37
10	Combination of AFM topography scans of collagens and cells on muscovite mica after 22.5 hours of cell seeding.	38
11	AFM topography of collagens and cells on non-cross-linked collagens on phlogopite mica after 22 hours of cell seeding.	38
12	AFM topography of collagens and cells on cross-linked collagens on phlogopite mica after 23 hours of cell seeding.	39

CHAPTER I

INTRODUCTION*

Cellular system exhibits two contradictory properties: robust and dynamic, where robust architecture is required for cells' survival while dynamic plasticity reflects the ability of cells to adapt to changing environment[1]. Microenvironment of cells is composed of other cells, the extracellular matrix (ECM), and various molecular factors which are involved in cell signaling. Cells constantly interact and remodel the surroundings via biochemical and biomechanical feedback loops to achieve homeostasis, which is critical to their survival. The complex interactions between cells and the extracellular microenvironment define various physiologial and pathological events including tissue morphogenesis[2], wound healing[3], and cancer cell metastasis[4]. Micromechanics of the ECM have shown to tremendously impact cell behaviors and functions as much as soluble factors do[5,6]. Physical parameters such as matrix geometry and stiffness can significantly affect cell survival[7], polarity[8], migration[9–11], proliferation[12], and differentiation[6,13]. Meanwhile, cells constantly modify and restructure the ECM[14], leading to a complex interdependency between cells and the ECM. Therefore, it is crucial to understand this intricated interactions between cells and the ECM for better apprehension of how they function together in forming complex tissues.

This thesis follows the style and format of *Nature*.

*Part of this chapter is reprinted with permission from Leow, W. W. and Hwang, W. Epitaxially guided assembly of collagen layers on mica surfaces. *Langmuir* **27**(17), 10907–10913 (2011). Copyright (2011) American Chemical Society.

A. Ordered two-dimensional collagen layers

Collagen type I is the major component of ECM. It forms fibrillar structure and is an extremely versatile tissue scaffold. Collagens self-assemble in a hierarchical manner to form ordered arrays in the extracellular matrix such as cornea, tendon, bone, and cartilage[15–19]. Collagens can also self-assemble *in vitro*, and the resulting matrices are used as two- and three-dimensional scaffolds for cells[20,21], to coat non-biological surfaces for enhanced bio-compatibility[22], for functionalized surface patterning[23,24], and even in microelectronics applications as a template for generating silicon nanowires[25]. Better understanding and control of the self-assembly process of collagen thus has both fundamental and practical importance.

In an earlier research, we use atomic force microscopy (AFM) to study the self-assembly process of collagen on flat substrates[26]. On muscovite mica, which is the most widely used substrate for AFM, collagens show a variety of assembly morphology depending on the pH and electrolyte composition of the buffer[27,28]. Under certain conditions, unidirectionally aligned layer of collagen forms with the D-periodic band[27,29]. Hereafter, we refer a D-periodic band simply as a D-period. Formation of a D-period indicates collagen molecules in a fibril are ordered in a native-like manner[30]. We then compare assembly of collagen on muscovite mica with that on a less widely used phlogopite mica, where the latter is known to preserve the surface hexagonal symmetry whereas muscovite does not[31,32]. On phlogopite, collagens assembled into a novel triangular network where individual fibril possesses a D-period. By comparing changes in the assembly morphology on both types of mica at different KCl concentrations, we find that K^+ affects the assembly by binding to the mica, which reduces the binding affinity of collagen and enhances surface diffusion of the weakly adsorbed collagen molecules. These results suggest that the assembly of collagen on mica oc-

curs via the initial adsorption to mica, surface diffusion, nucleation and growth into a two-dimensional network of fibrils. The mica lattice determines the growth direction of fibrils during the nucleation step, while potassium affects surface adsorption and diffusion of collagen molecules by neutralizing the mica surface.

B. Cell adhesion via mechanotransduction

Cells sense and relate to the physcial environment using a phenomenon known as mechanotransduction. Mechanotransduction are based on various physical aspects, but the molecular mechanisms underlying each system are rather specific[33]. Cell attachment to the ECM is the first and most crucial criteria to the complex cell-matrix interactions. Most evidence suggests that cells utilize integrin-based sites of adhesion, or focal adhesion, in its mechanotransduction process for rigidity sensing and to mediate force transmission from cell to subtrate[34,35]. Focal adhesion serves as the intermediate which links intracellular actin cytoskeleton and the ECM. It has two major functions: (i) to provide structural support to maintain adhesion to substrate and (ii) to serve as strong signaling center to activate many important signaling cascades[36]. ECM contains specific domains which serve as the ligands for integrin binding. As illustrated in Fig. 1, cell adhesion involves activation of integrins by binding with the ECM, while the intracellular domains of integrins are bound to actin cytoskeleton via adaptor proteins such as talin, α-actinin, filamin, and vinculin. Recruitment of intracellular signalling proteins, such as focal adhesion kinase (FAK) at this integrin-adapter protein-cytoskeleton complex forms the basis of adhesion complexes, which then mature into focal adhesions with clustering of integrins to increase their avidity and further increased integrin packing density. Mature adhesion often acts as a checkpoint for critical celllular decisions, such as migration, proliferation, and also matrix

remodeling which leads to change in tissue mechanics, thus generating the feedback loops between the cell and its microenvironment[33].

C. Cellular remodeling of ECM

Many previous studies of cell-matrix interactions have been performed on different artificial cell-culture substrates to illustrate how changes in cellular behaviors are correlated to matrix mechanical properties[12,37–39]. Wrinkles observed on the thin elastic substrate was evidence of deformation generated by cell contractility[37]. More recently, two-dimentional collagen layers were developed to study cell-matrix interactions, where parallelly aligned collagen fibrils were self-assembled on mica under optimum salt and pH conditions[21,26,40]. Friedrichs et al. showed that human osteoblast-like cells (SAOS) can polarize on aligned collagen layers with D-period, but not on cross-linked layers, or layers without D-period[21]. In Fig. 2, upon cell seeding, protrusions are formed in all directions as cells sample the surrounding. As adhesion complexes formed, cells begin to exert pulling forces in all directions. Non-periodic collagen fibrils are mechanically weak and thus rupture as cells pull, whereas on matrix with aligned collagen fibrils with D-period, cells are able to establish strong traction along the direction of fibrils, while high pliability in the direction perpendicular to fibril alignment, hence resulting in cell polarization in the direction of fibril alignment. Cross-linked collagen layers provide isotropic traction to cells and hence cells cannot polarize. The role of integrin $\alpha_2\beta_1$ in cell attachment and alignment on collagen layers were demonstrated in this study, along with other studies using retinal pigment epithelium cell[41], corneal endothelial cell[42], and human melanoma cell[43]. Besides, cell shape and alignment index were analyzed using phase contrast images[41,42]. The aligned collagen layers were used to study the dependency of proteolysis on cell ad-

hesion to the matrix and force generation[43]. Combining fluorescence microscopy and AFM, the study shows blocking of integrin $\alpha_2\beta_1$ (cell adhesion), actin polymerization and myosin II (force generation and rigidity sensing) effectively lowers the proteolysis of collagen layers by cells.

In this study, 2D aligned and triangular-patterned collagen layers capable of supporting cells are created, while the methods and proposed theory will be discussed here. We use Fluoresence Microscopy and AFM to elucidate the change in cell shape in relation to the matrix deformation on these collagen layers. 2D ordered collagen layers serve as an excellent model to study matrix remodeling as it resembles the ordered ECM environment in tissues such tendon and cornea. It also allows deformation of individual collagen fibrils to be visualized under AFM, making quantification of matrix deformation possible.

CHAPTER II

MATERIALS AND METHODS*

The overview of the experimental procedures is illustrated in Fig. 3. A freshly cleaved mica disk was first placed at the center of glass bottom petri dish and affixed by applying vacuum grease at the mica edges contacting the petri dish. Collagen-buffer solution was then deposited onto the mica and incubated overnight to allow formation of 2D ordered collagen layers. Collagens assembled into parallel aligned fibrils on muscovite mica while triangular network on phlogpite mica. After flushing the mica with Phosphate Buffered Saline (PBS), sample was UV-sterilized and seeded with U2OS cells. Sample was then incubated overnight at 37°C and subjected to Fluorescence and AFM imaging after fixing. The transparent mica and glass bottom petri dish setup allows Light and Fluorescence Microscopy to be possible.

A. Preparation of ordered 2-D collagen layers

Collagen stock was prepared using solubilized type I collagen derived from rat tail tendon (BD Biosciences 354236) (3.74 mg/ml) with >90% purity by SDS-PAGE. The stock was diluted with 0.1% acetic acid to 1.65 mg/ml (pH 2.5) and stored at 4°C, and was used for experiments for up to 3 months. Collagen sample was prepared from collagen stock diluted with a buffer to a given concentration, containing 30 mM Na_2HPO_4, 10 mM KH_2PO_4, and optionally 50 mM glycine, at pH 7. The buffer also contained KCl at 200 mM for samples on muscovite mica and 150 mM for phlogopite mica.

---

*Part of this chapter is reprinted with permission from Leow, W. W. and Hwang, W. Epitaxially guided assembly of collagen layers on mica surfaces. *Langmuir* **27**(17), 10907–10913 (2011). Copyright (2011) American Chemical Society.

12 mm muscovite mica disks (Grade V1) were purchased from Ted Pella, Inc. (CA, USA) and phlogopite mica sheets were custom-ordered from Axim Mica (NY, USA). A mica sheet was freshly cleaved by sticky tape or lifting with razor blade to ensure clean surface before each experiment. Mica was placed atop a 50 mm uncoated glass bottom (No. 0) petri dish (MatTek Co., Ashland, MA) with silicone high vacuum grease (Dow Corning) applied around the mica edges to avoid sample drifting. For samples used for direct AFM imaging, mica was affixed on a metal disk with double sided tape. A 70-μl aliquot of the collagen sample solution was deposited on mica and incubated at room temperature overnight (>10 hours) in a moisture chamber to minimize evaporation.

To prepare cross-linked collagen layers, microbial transglutaminase (mTG) was obtained from Dr. A. Yeh's lab as a generous gift, inially at 16.67 mg/ml and stored at -20°C. Prior to cross-linking, mTG aliquot was diluted with collagen buffer to 0.67 mg/ml. Collagen sample on mica was flushed multiple times in multiple directions with collagen buffer, followed by 70-μl mTG solution deposition. The sample was then incubated at room temperature for >10 hours in a moisture chamber.

Before AFM imaging, all samples were gently flushed multiple times with deionized water in multiple flow directions. The mica was then carefully affixed on a metal disk with double sided tape. Kimwipes were used to carefully remove excess water from the edges of mica. The mica disk was then left to air-dry for more than 10 minutes in ambient conditions (room temperature), half-covered with a plastic dish. The dried sample was used for AFM imaging.

B. Cell culture

U2OS osteosarcoma cells stably expressing GFP-actin (MarinPharm GmbH) were used between passages 2 and 15 and subcultured in DMEM (GIBCO) supplemented with 10% fetal bovine serum, 2 mM L-glutamine, 1 mM sodium pyruvate and 1 mM penicillin-streptomycin in a humidified 5% CO_2 incubator kept at 37°C. Cells were passaged every 2 to 4 days.

C. Cell seeding and fixing

Prior to cell seeding, all collagen samples were flushed with 1X PBS multiple times in multiple directions. Samples were then incubated in 1X PBS and sterilized under UV radiation for 30 mins. Cell seeding was performed under sterile condition. Cells were at 70%–90% confluence. Cell were trypsinized and roughly a total of 100–200 μl of 20% cells were added to 7 ml medium in the petri dish containing collagen-coated mica. Petri dish was then incubated at 37℃ in 5% CO_2 incubator for >24 hours to allow cell attachment and spreading.

Prior to fluorescence imaging and AFM, cells were fixed under sterile condition to avoid bacterial growth on samples. Cells were washed with sterilized 1X PBS, followed by fixing with ice-cold 2% (v/v) glutaldehyde/PBS for 1 min, and ice-cold 4% (v/v) paraformaldehyde/PBS for 30 mins. Samples were then washed extensively with 1X PBS and used immediately or stored at 4℃.

D. AFM imaging

The AFM (Veeco CP-II, CA, U.S.A.) was operated in air at room temperature with a 100×100 μm^2 piezoelectric large area scanner. Antimony doped silicon probe (Veeco Probes, FESP7) with a nominal force constant of 2.8 N/m was used. Imaging was

performed in the non-contact tapping mode (NCM) with a driving frequency near the the nominal resonance frequency of the cantilever ($\sim$75 kHz). The NCM amplitude was maintained at about 70 nm, the signal to noise ratio was higher than 10, and the gain ranging from 0.1–0.3. The scanning speed was 1 Hz for small-area scans ($<$2 μm) and decreased when scanning larger areas to ensure image quality.

Image analysis and processing were performed in the di-SPMLab software. Only basic image processing including leveling and adjustment to the contrast histogram were done. Line analysis was performed to measure heights and lengths of collagens. Fibril height was averaged over 10 measurements and the length of a D-period was obtained from an average over 10 measurements where each measurement was on a straight region of a fibril with about 10 pitches. Data are presented as [average$\pm$standard deviation].

CHAPTER III

RESULTS*

A. Formation of 2D collagen layers

Collagen assembly on a flat substrate follows the surface adsorption, diffusion, nucleation, and growth pathway[26]. Collagens assemble into parallel aligned fibrils on muscovite mica, while triangular networks are formed on phlogopite mica. Layers morphology is sensitive to buffer conditions and collagen concentration, particularly changing the potassium concentration affects the assembly of collagen molecules on mica. Addition of glycine was found to be necessary for collagen layers to be capable of supporting cells. Cross-linking the layers with mTG creates an alternative matrix with isotropic tensile strength to study cellular behaviors.

1. Assembly of unidirectionally aligned collagen layers on muscovite mica

Muscovite mica is a phyllosilicate mineral of aluminium and potassium, with a common chemical formula $KAl_2(AlSi_3O_{10})(F,OH)_2$. Mica has several outstanding properties which make it an excellent substrate for AFM and Electron Microscope. Basal cleavage of mica yields a very even, flat, and clean surface for high resolution imaging. Muscovite is lightly brown-tinted, but allows sufficient light transmission for Fluorescence Microscopy.

In our earlier study, highly aligned collagen fibrils were observed within 1 minute of incubation on muscovite mica with 10 μg/ml collagen and 200 mM KCl (without glycine)[26]. To understand the mechanism for the appearance of order, we observed

---

*Part of this chapter is reprinted with permission from Leow, W. W. and Hwang, W. Epitaxially guided assembly of collagen layers on mica surfaces. *Langmuir* **27**(17), 10907–10913 (2011). Copyright (2011) American Chemical Society.

collagen assembly at a concentration of 0.5 μg/ml, well below the critical concentration for collagen fibrillogenesis in bulk solution (4.73 μg/ml at 29 °C)[44]. With 200 mM KCl, we incubated the solution on mica for various durations and imaged with AFM (Fig. 4). At 1 minute, randomly adsorbed molecules are visible (Fig. 4a). They are approximately 230–320 nm in length, corresponding to the length of a single collagen molecule[30,45]. At 18 minute, straight collagen fibrils appear, corresponding to nucleation events (Fig. 4b, arrow), which become more abundant and grow in size by 30 minute incubation (Fig. 4c). Their height is 1.1±0.15 nm, consistent with a single-molecule thick layer. Although D-periodic bands are visible (Fig. 4d), the periodicity is 88.3±11.97 nm (measured over 4 filaments in 2 images), again indicating that the molecules in a fibril do not have the native-like packing at this stage.

Since sub-critical concentration of collagen was used, formation of the nascent fibrils as in Fig. 4b in solution before deposition onto mica was unlikely. The fibrils appear in parallel with distances comparable to or larger than their own lengths, which precludes an alignment mechanism due to the liquid crystalline behavior of collagen as observed in tissues or at very high concentrations (>20 mg/ml)[46–48]. Initial random adsorption of collagen molecules and dependence of the assembly process on the incubation time on mica also exclude the possibility of alignment due to hydrodynamic flow induced when the solution is deposited on mica. Considering these factors, the most likely mechanism for the alignment is guidance by the underlying mica lattice.

2. Formation of triangular collagen networks on phlogopite mica

Phlogopite, also known as magnesium mica due to its chemical structure ($KMg_3(AlSi_3O_{10}(F,OH)_2)$), is a less commonly used substrate. It has a more opaque appearance with poor light transmittance compare to muscovite and therefore making Fluorescence Microscopy difficult.

Compare to muscovite, which is a dioctahedral mica possessing a tetrahedral tilt, phlogopite is a trioctahedral mica with less lattice distortion[31,32,49]. This causes muscovite to possess a surface lattice with broken hexagonal geometry while the surface geometry is perserved in phlogopite. With 150 mM KCl, collagens assembled on phlogopite into an extensive triangular network (Fig. 5a). Collagen fibrils also had the native-like 67-nm D-period and longer ones bent along the triangular pattern (Fig. 5(a)). The height of the fibrils were 7.08±1.87 nm, which is much greater than that on muscovite mica under the same condition (1.79±0.37 nm). This is likely because collagens bundle more extensively since they have a lower affinity for phlogopite than for muscovite.

3. Layers morphology depends on potassium concentration

Concentration of the potassium, as one of the key ingredients in the buffer, was observed to have profound effects on collagen morphology[26]. We varied concentration of KCl and compared morphologies of the collagen network on muscovite and phlogopite after 30-min incubation (Fig. 6). At 50 mM KCl, a checkerboard-like pattern emerged on muscovite whereas on phlogopite individual fibrils arranged into a triangular pattern (Fig. 6a,b). Compared to muscovite, less collagens adsorbed to phlogopite and fibrils grew longer, indicative of a lower affinity and higher surface diffusion of collagen molecules on phlogopite. On muscovite, due to the lower level of diffusion, two directions of growth may be possible as collagen oligomers at the pre-nucleation stage ('protofibrils') may not be able to rotate to energetically the most favorable direction. Consistent with this, a small number of collagen fibrils grow in the third direction (arrow in Fig. 6a). At 100 mM KCl, extensive alignment occurs on muscovite, suggesting that protofibrils of collagen are able to rotate and find the most favorable direction on mica (Fig. 6c). The enhanced surface diffusion manifests as extensive

bundling of fibrils on phlogopite (Fig. 6d). Finally, at 400 mM KCl, likely due to the even higher level of diffusion, collagen molecules and oligomers coalescented into fewer fibrils (Fig. 6e). Presence of a D-period also suggests that collagen molecules diffuse axially after forming the fibril. On the other hand, no extensive growth was observed on phlogopite (Fig. 6f). The already weak interaction between collagen and phlogopite may have been reduced further by neutralization of mica by the surface-bound K^+. Only small aggregates are present, which may be either collapsed monomers or oligomers. They could be in adsorption-desorption equilibrium with the incubating solution, or may eventually nucleate fibrils with a prolonged incubation time. These results indicate that binding of K^+ on mica reduces adsorption and enhances surface diffusion, which in turn affect the morphology of the collagen layer. Our experiments also suggest that the optimal KCl concentration for extensive ordering of collagen fibrils with a D-period is 200–400 mM on muscovite and ∼150 mM on phlogopite.

4. Addition of glycine and cross-linking with mTG

Addition of glycine (50 mM) along with collagens created rounder fibrils. Fig. 7 compares collagens formed without glycine (Fig. 7(a)) and with glycine (Fig. 7(b)) on muscovite mica. Fibril height was measured to be 6.11±2.18 nm without glycine and 12.71±2.01 nm with glycine (Fig. 7(c)). In both cases, the periodicity was almost similar (∼68 nm). Samples without glycine failed to sustain incubation in buffer or cell culture media for more than 2 hours, likely due to hydrolytic degradation of collagens. Addition of glycine to to the collagen-buffer mixtures allows formation of more defined collagen layers and enables cell experiments.

On phlogopite mica, fibrils in samples with glycine (Fig. 5b) were observed to be able to “crawl” over an existing fibril, creating a less defined triangular network. Cross-linking collagens on phlogopite with mTG was found to have minimal effect on

altering the collagen morphology (Fig. 5c). In this study, mTG was directly added to the well formed collagen fibrils and incubated for more than 10 hours to form cross-linked networks. According to a study, in order for mTG to cross-link collagens, the collagen triple helix has be to unwound to allow exposure of lysine and glutamine residues[50]. Our results indicate that this is not necessary and collagens get to remain undenatured upon mTG cross-linking.

B. Cell-matrix interactions

1. Anisotropic cellular remodeling of collagen layers on muscovite

Aligned collagen layers formed on muscovite mica were observed to extend their parallel structure over a large area (at least 100 μm^2). These extensively parallel fibrils possess high tensile strength along the direction of fibril alignment, and high pliability perpendicular to the alignment direction[21]. Also, compared to non-periodic collagens which are known to be weak[21], these fibrils possess D-periods which resembles their native-like structure, therefore making them a highly anisotropic matrix. We observed fibrils deformation in the direction perpendicular to the alignment direction as a result of pulling forces between two U2OS cells, as shown in Fig. 8(a). Fig. 8(b) shows a zoom-in scan of the deformed collagens, where the inset indicates presence of D-periods on the fibrils.

In another experiment, we imaged U2OS cells on anisotropic collagen layers using fluorescence microscopy. Fig. 9 shows a typical fluorescence image of U2OS cells on non-cross-linked collagen layers on muscovite, under 20X objective. Cell density was high. Stress fiber can be observed as bright straight lines on the image. Cells appeared to be well spreaded, with majority of the cells polarized in one direction, which is likely the direction of collagen alignment. To better illucidate the cell-matrix interactions,

we used AFM to scan different areas on the sample. It was rather difficult to capture one single cell spreaded on the matrix due to the high cell density and scan size limit of the AFM. Therefore, combination of AFM scans were produced as a way to speed up the "search and scan" process, aided by the close-loop AFM scanner with the capability to track the x and y positions of the scans. Shown in Fig. 10 are two big AFM images produced by carefully combining scans of the adjacent areas. Cells could clearly deform the aligned collagen layers. Part of some cells were observed to penetrate underneath the collagen layers while some formed protrusions over the matrix. Stress fiber-like strcutures were observed (Fig. 10a) on some of the cells. Cells were also able to bundle the collagen fibrils during deformation, as shown in Fig. 10b.

2. Cells on triangular collagen networks on phlogopite

Prior to cross-linking, we failed to observe collagen layers after cells were seeded on the triangular collagen networks on phlogopite, shown in Fig. 11. Collagen layers were likely being completely deformed by cells, as we tested the capability of the collagen layers in surviving pro-longed liquid incubation and chemical fixing. To enhance the strength of these triangular networks, mTG was used to provide specific enzymatic cross-links on the layers. Cross-linking with mTG did not change the morphology of the triangular network, as indicated in Fig. 5(c). U2OS cells were then seeded on cross-linked triangular collagen matrix on phlogopite, and we observed the matrix remained undeformed after 23 hours of cells seeding (Fig. 12). Cells appeared to be rounder compared to the polarized cells on muscovite. Also, cells formed protrusions which followed one of the three directions of the collagen fibrils (Fig. 12b).

CHAPTER IV

DISCUSSION*

A. Formation of 2D collagen layers

Collagens assemble on mica through a similar pathway as in bulk solution, where collagen molecules first adsorb, perform surface diffusion, nucleate a fibril, and grow[26]. The initial adsorption is mediated by van der Waals forces as a whole, and more locally the electrostatic interactions between and the positively charged side chains and the partially negatively charged mica surface. Formation of uniaxial collagen fibrils was initially attributed to hydrodynamic flow upon collagen deposition on mica[27], but another study suggested that collagen alignment on mica is quasi-epitaxial, induced by the crystallographic orientation of the mica surface[51]. The results of our study supports the latter. Different assembly morphologies on muscovite and phlogopite unambiguously show that the growth direction of collagen fibrils is guided by the underlying mica lattice. On phlogopite, the triaxial fibrils clearly indicates that the order is not generated by hydrodynamic flow or liquid crystalline behaviors. Understanding the lattice structure of mica will help explain epitaxy effect in mica and the role of K^+ in affecting molecules assembly. On muscovite mica, replacement of Si^{4+} by Al^{3+} renders the surface to be negatively charged, which is compensated for by K^+[52,53]. The distortion of the lattice on muscovite[31,32,49,54] is caused by the tilting of the OH group in the octahedral sheet. Also, the OH tilt results in longer O–H$\cdots$K$^+$ distance in muscovite compare to phlogopite. With the H atom in the hydroxyl group having a partial positive charge, K^+ binds less strongly to phlogopite[55],

*Part of this chapter is reprinted with permission from Leow, W. W. and Hwang, W. Epitaxially guided assembly of collagen layers on mica surfaces. *Langmuir* **27**(17), 10907–10913 (2011). Copyright (2011) American Chemical Society.

which is consistent with the weaker binding and higher thickness of collagen fibrils on it. Moreover, for muscovite, K^+ preferentially binds to lattice sites with two underlying Al atoms rather than those with one Al atom, which results in lining up of K^+ on alternating rows of the mica lattice[56]. This may provide additional guidance in the unidirectional alignment of collagen where individual molecules locate between the rows of K^+ and their positively charged side chains[57] interact with the K^+-binding pockets of mica.

However, the mechanism by which mica guides the growth direction of the large and flexible collagen molecules is unclear. A single collagen molecule is a triple helix of α-chains, $\sim$1.4-nm in diameter and 300 nm in length[45]. By comparison, unit cells of the surface lattice in muscovite and phlogopite mica are about 0.5×0.9 nm^2 (a$\times$b)[32]. Earlier studies show the presence of surface electric dipole field on muscovite that is 75° relative to the high-symmetry direction of the lattice[49,53]. Smaller molecules such as *para*-hexaphenyl (a linear chain of six phenyl rings) aligns with the dipole field and assemble laterally in the [110] and [1$\bar{1}$0] directions of the mica lattice[49,58], where individual molecules orient 15° with respect to filament axis. Similarly, Aβ25-35 that also exhibits an epitaxial growth on mica[59,60], forms the so-called amyloid 'cross-β' structure where each peptide is perpendicular to the fibril axis[61]. On the other hand, collagen assembly in stagger manner and molecules lie along the length of a fibril. If collagen fibrils align with one or more of the symmetry axes of the mica lattice[51], it will thus be nearly perpendicular to the surface dipole field, whose role in guiding the alignment is unclear. Presence of surface groove on muscovite mica due to its broken hexagonal symmetry[31,32,49] could also potentially induce alignment of collagens. Nonetheless, the groove is only 0.7–0.8 Å in depth, nearly 1/20 of the diameter of a collagen molecule. Hence, its role in the alignment of collagen fibrils would be minor. In reality, it is likely that the growth direction is determined by the

interplay between multiple factors, including surface topography and electrostatics.

Dependence of collagen morphology on potassium concentration was rather specific to mica. Within the mica lattice there is a layer of potassium atoms between silicate sheets that becomes the cleavage plane[53]. Since about half of potassium atoms will be removed after cleavage, there will be empty potassium binding pockets, resulting in a partially negatively charged surface. On the other hand, collagen molecules (pI 9.3[27]) are positively charged at neutral pH. Therefore, if the buffer contains insufficient amount of K^+ ions, collagen molecules will adsorb more strongly to the mica and diffuse less. On muscovite mica, specificity of K^+ in affecting molecules assembly has been demonstrated in the case of the 10-residue long Aβ25-35 peptide[59,60]. They assembled into fibers in three directions on muscovite mica. At higher concentration of cations, adsorption was reduced and filaments did not form. For the inhibitory effect, about 10-fold less KCl was required than NaCl, suggesting that K^+ binds more tightly to the mica surface[60]. This also shows that Cl^- does not significantly affect the binding affinity to the mica surface[40]. The mechanism by which glycine protected collagen molecules from hydrolytic degration was unclear. One postulation is that glycine increases the solution viscosity, and possibly changes the surface energy of the collagen fibril, thereby stabilizes the collagen assembly. Addition of glycine to collagens formed rounder and more defined fibrils which can sustain chemical treatment such as fixing. The well-formed collagen layers can then be used to study cell-matrix interactions.

B. 2D collagen layers as a model to study cell-matrix interactions

Upon attachment, cells exert pulling forces in all directions in stay in tension. On anisotropic collagen layers on muscovite, fibrils were deformed in the direction per-

pendicular to the alignment direction due to low tensile strength as opposed to the alignment direction. As a result, cells are expected to polarize in the direction of fibril alignment[21]. Fluorescence image shows the presence of stress fibers on U2OS cells seeded on the non-cross-linked parallel collagen layers (9). Formation of stress fibers indicates cells are in tension. Stress fibers also indicate focal adhesion formation, which is important in regulating cell signaling. In our results (Fig. 9 and Fig. 10), not all cells polarize in the direction of fibrils alignment. Especially in Fig. 10, the directions of cells polarization were rather random. Stress fibers were observed to polarize in some cells, while randomly formed in others (Fig. 9). One postulation is that cells were overcrowded. As one cell deforms the matrix from one direction, another cell near-by tries to pull on the same fibrils, which are now distorted from their original alignment and therefore cannot provide high tensile strength in the original alignment direction, resulting in cell polarization in various directions around the alignment axis. Similar explanation can applied to cells which were observed to be less polarized, where majority of the surrounding matrix might be dirupted by neighboring cells. As a precaution to future experiment, lower cell density should be used to clearly visualized the cellular remodeling of collagen layers.

Cell-matrix entanglement can be observed as cells extended their protrusions over and penetrated below the collagen layers during the cellular remodeling process (Fig. 10). This complex entanglement of cells and collagen fibrils were observed in previous study[21], and for fibroblasts in 3D collagen matrices where it enhanced mechanical cell attachment to 3D collagen matrices[62]. Therefore, cells might achieve enhanced traction by encompassing the thin collagen fibrils, by increasing cell-matrix contacts.

Non-cross-linked triangular collagen networks on phlogopite did not survive cell pulling due to its geometry. These triaxial fibrils are generally short, and do not con-

nect to each other, therefore fail to sustain cell pulling forces. Hence, cross-linking the triangular networks with mTG allows these fibrils to connect to each other and create an isotropic network which can survice cell pulling. In general, cells appeared rounder which could be explained by uniform tensile strength of the isotropic matrix. Due to the opaque apperance of phlogopite mica, fluorescence imaging became impossible with the inverted microscope setup we have, even with very thin layer of mica sheet. Cells formed protrusions along the directions of fibril directions on phlogopite which can be attributed to contact guidance. Protrusions are formed when cells need to make transient adhesions, sample the environment, or during cell locomotion at the leading edge[63]. It is of vast interest to observe how cells determine which one of the three directions to form protrusions and hence migrate on the triangular network. Further investigation has to be performed to confirm.

2D collagen substrates are generally used for tissue culture coatings and are generally not suitable for cell growth due to the flat and rigid surfaces which do not resemble natural tissues. However, the 2D collagen layers created in this study provide an excellent model to elucidate cell-matrix interactions on ordered matrices and allows matrix remodeling to be visualized at high resolution. Furthermore, the formation of cell-matrix entanglement on 2D collagen layers resembles similar structures used to enhance anchorage of cells to ECM in 3D, thereby suggesting the cell-matrix interactions on 2D collagen layers may involve a considerable 3D component[21].

CHAPTER V

SUMMARY AND CONCLUSION

In this study, two-dimensional ordered collagen layers were created on mica. Parallel aligned collagen fibrils were formed on muscovite mica while triangular collagen networks were formed on phlogopite mica. Assembly of these colagen layers were epitaxially guided, which in general followed the adsorption, surface diffusion, nucleation, and growth pathway. Balance of adsorption and surface diffusion by controlling potassium ion concentration could change the morphology of collagens on both muscovite and phlogopite. These 2D ordered collagen layers were then used to study cell-matrix interactions. On muscovite mica, aligned collagen layers provide anisotropic traction for cells. Cells were observed to polarize in the direction of fibrils alignment and formed stress fibers. Collagens were deformed and bundled as cells extended over and penetrated under the collagen layers during matrix remodeling process. On phlogopite mica, cells deformed the untreated triangular networks completely. After cross-linking, triangular collagen networks provide isotropic traction and cells did not polarized. Cells also formed protrusions along the fibrils directions. In a nutshell, the 2D ordered collagen layers serve as an excellent model to study cell-matrix interactions in which high resolution images of cellular remodeling of collagen layers provide useful information about the complex relationship between cells and the ECM.

REFERENCES

[1] Gardel, M. and Schwarz, U. Preface for cell–substrate interactions. *Journal of Physics: Condensed Matter* **22**, 190301 (2010).

[2] Lecuit, T. and Lenne, P. F. Cell surface mechanics and the control of cell shape, tissue patterns and morphogenesis. *Nature Reviews Molecular Cell Biology* **8**(8), 633–644 (2007).

[3] Ehrlich, H. Wound closure: Evidence of cooperation between fibroblasts and collagen matrix. *Eye* **2**(2), 149–157 (1988).

[4] Liotta, L., Tryggvason, K., Garbisa, S., Hart, I., Foltz, C., and Shafie, S. Metastatic potential correlates with enzymatic degradation of basement membrane collagen. *Nature* **284**(5751), 67–68 (1980).

[5] Chen, C. S., Mrksich, M., Huang, S., Whitesides, G. M., and Ingber, D. E. Geometric control of cell life and death. *Science* **276**(5317), 1425 (1997).

[6] Discher, D. E., Janmey, P., and Wang, Y. Tissue cells feel and respond to the stiffness of their substrate. *Science* **310**(5751), 1139 (2005).

[7] Critser, P. J., Kreger, S. T., Voytik-Harbin, S. L., and Yoder, M. C. Collagen matrix physical properties modulate endothelial colony forming cell-derived vessels in vivo. *Microvasc. Res.* **80**(1), 23–30 (2010).

[8] Théry, M., Racine, V., Piel, M., Pépin, A., Dimitrov, A., Chen, Y., Sibarita, J. B., and Bornens, M. Anisotropy of cell adhesive microenvironment governs cell internal organization and orientation of polarity. *P. Natl. Acad. Sci.* **103**(52), 19771 (2006).

[9] Jiang, X., Bruzewicz, D. A., Wong, A. P., Piel, M., and Whitesides, G. M. Directing cell migration with asymmetric micropatterns. *P. Natl. Acad. Sci. USA* **102**(4), 975 (2005).

[10] Zaman, M. H., Trapani, L. M., Sieminski, A. L., MacKellar, D., Gong, H., Kamm, R. D., Wells, A., Lauffenburger, D. A., and Matsudaira, P. Migration of tumor cells in 3d matrices is governed by matrix stiffness along with cell-matrix adhesion and proteolysis. *P. Natl. Acad. Sci.* **103**(29), 10889 (2006).

[11] Lehnert, D., Wehrle-Haller, B., David, C., Weiland, U., Ballestrem, C., Imhof, B. A., and Bastmeyer, M. Cell behaviour on micropatterned substrata: limits of extracellular matrix geometry for spreading and adhesion. *J. Cell Sci.* **117**(Pt 1), 41–52 (2004).

[12] Khatiwala, C. B., Peyton, S. R., and Putnam, A. J. Intrinsic mechanical properties of the extracellular matrix affect the behavior of pre-osteoblastic mc3t3-e1 cells. *Am. J. Physiol.- Cell Ph.* **290**(6), C1640 (2006).

[13] Engler, A. J., Sen, S., Sweeney, H. L., and Discher, D. E. Matrix elasticity directs stem cell lineage specification. *Cell* **126**(4), 677–689 (2006).

[14] Vogel, V. and Sheetz, M. Local force and geometry sensing regulate cell functions. *Nat. Rev. Mol. Cell Bio.* **7**(4), 265–275 (2006).

[15] Cowin, S. How is a tissue built? *J. Biomech. Eng.* **122**, 553 (2000).

[16] Ushiki, T. Collagen fibers, reticular fibers and elastic fibers. A comprehensive understanding from a morphological viewpoint. *Arch. Hist. Cytol.* **65**(2), 109–126 (2002).

[17] Holmes, D. F., Gilpin, C. J., Baldock, C., Ziese, U., Koster, A. J., and Kadler, K. E. Corneal collagen fibril structure in three dimensions: Structural insights into fibril assembly, mechanical properties, and tissue organization. *Proc. Natl. Acad. Sci. USA* **98**(13), 7307–7312 (2001).

[18] Cui, F. Z., Li, Y., and Ge, J. Self-assembly of mineralized collagen composites. *Mat. Sci. Eng. R.* **57**(1-6), 1–27 (2007).

[19] Banos, C. C., Thomas, A. H., and Kuo, C. K. Collagen fibrillogenesis in tendon development: current models and regulation of fibril assembly. *Birth Defects Res. C* **84**(3), 228–244 (2008).

[20] Thomas, A. C., Campbell, G. R., and Campbell, J. H. Advances in vascular tissue engineering. *Cardiovasc. Pathol.* **12**(5), 271–276 (2003).

[21] Friedrichs, J., Taubenberger, A., Franz, C. M., and Müller, D. J. Cellular remodelling of individual collagen fibrils visualized by time-lapse AFM. *J. Mol. Biol.* **372**(3), 594–607 (2007).

[22] Lee, C. H., Singla, A., and Lee, Y. Biomedical applications of collagen. *Int. J. Pharm.* **221**(1-2), 1–22 (2001).

[23] Monroe, M. R., Li, Y., Ajinkya, S. B., Gower, L. B., and Douglas, E. P. Directed collagen patterning on gold-coated silicon substrates via micro-contact printing. *Mater. Sci. Eng.-C* **29**, 2365–2369 (2009).

[24] Zhu, B., Lu, Q., Yin, J., Hu, J., and Wang, Z. Alignment of osteoblast-like cells and cell-produced collagen matrix induced by nanogrooves. *Tissue Eng.* **11**(5-6), 825–834 (2005).

[25] Salhi, B., Vaurette, F., Grandidier, B., Stiévenard, D., Melnyk, O., Coffinier, Y., and Boukherroub, R. The collagen assisted self-assembly of silicon nanowires. *Nanotechnology* **20**, 235601–235607 (2009).

[26] Leow, W. W. and Hwang, W. Epitaxially guided assembly of collagen layers on mica surfaces. *Langmuir* **27**(17), 10907–10913 (2011).

[27] Jiang, F., Hörber, H., Howard, J., and Müller, D. J. Assembly of collagen into microribbons: effects of ph and electrolytes. *J. Struct. Biol.* **148**(3), 268–278 (2004).

[28] Li, Y., Asadi, A., Monroe, M. R., and Douglas, E. P. ph effects on collagen fibrillogenesis in vitro: Electrostatic interactions and phosphate binding. *Mat. Sci. Eng. C* **29**(5), 1643–1649 (2009).

[29] Cisneros, D. A., Hung, C., Franz, C. M., and Müller, D. J. Observing growth steps of collagen self-assembly by time-lapse high-resolution atomic force microscopy. *J. Struct. Biol.* **154**(3), 232–245 (2006).

[30] Kadler, K. E., Holmes, D. F., Trotter, J. A., and Chapman, J. A. Collagen fibril formation. *Biochem. J.* **316**(Pt 1), 1–11 (1996).

[31] Kuwahara, Y. Muscovite surface structure imaged by fluid contact mode afm. *Phys. Chem. Miner.* **26**(3), 198–205 (1999).

[32] Kuwahara, Y. Comparison of the surface structure of the tetrahedral sheets of muscovite and phlogopite by afm. *Phys. Chem. Miner.* **28**(1), 1–8 (2001).

[33] Ludwig, T., Kirmse, R., Poole, K., and Schwarz, U. Probing cellular microenvironments and tissue remodeling by atomic force microscopy. *Pflug. Arch. Eur. J. Phy.* **456**(1), 29–49 (2008).

[34] Bershadsky, A. D., Balaban, N. Q., and Geiger, B. Adhesion-dependent cell mechanosensitivity. *Annu. Rev. Cell Dev. Bi.* **19**(1), 677–695 (2003).

[35] Geiger, B., Bershadsky, A., Pankov, R., and Yamada, K. M. Extracellular matrix–cytoskeleton crosstalk. *Nat. Rev. Mol. Cell Biol.* **2**, 793–805 (2001).

[36] Burridge, K. and Chrzanowska-Wodnicka, M. Focal adhesions, contractility, and signaling. *Annu. Rev. Cell Dev. Bi.* **12**(1), 463–519 (1996).

[37] Lee, J., Leonard, M., Oliver, T., Ishihara, A., and Jacobson, K. Traction forces generated by locomoting keratocytes. *J. Cell Biol.* **127**(6), 1957 (1994).

[38] Burton, K. and Taylor, D. L. Traction forces of cytokinesis measured with optically modified elastic substrata. *Nature* **385**(6615), 450–454 (1997).

[39] Kirchenbüchler, D., Born, S., Kirchgeßner, N., Houben, S., Hoffmann, B., and Merkel, R. Substrate, focal adhesions, and actin filaments: a mechanical unit with a weak spot for mechanosensitive proteins. *J, Phys.- Condens. Mat.* **22**, 194109 (2010).

[40] Loo, R. W. and Goh, M. C. Potassium ion mediated collagen microfibril assembly on mica. *Langmuir* **24**(23), 13276–13278 (2008).

[41] Ulbrich, S., Friedrichs, J., Valtink, M., Murovski, S., Franz, C. M., Müller, D. J., Funk, R. H. W., and Engelmann, K. Retinal pigment epithelium cell alignment on nanostructured collagen matrices. *Cells Tissues Organs* **194**(6), 443–456 (2011).

[42] Gruschwitz, R., Friedrichs, J., Valtink, M., Franz, C. M., Müller, D. J., Funk, R. H. W., and Engelmann, K. Alignment and cell-matrix interactions of human

corneal endothelial cells on nanostructured collagen type I matrices. *Invest. Ophth. Vis. Sci.* **51**(12), 6303–6310 (2010).

[43] Kirmse, R., Otto, H., and Ludwig, T. Interdependency of cell adhesion, force generation and extracellular proteolysis in matrix remodeling. *J. Cell Sci.* **124**(11), 1857 (2011).

[44] Kadler, K. E., Hojima, Y., and Prockop, D. J. Assembly of collagen fibrils de novo by cleavage of the type I pC-collagen with procollagen C-proteinase. Assay of critical concentration demonstrates that collagen self-assembly is a classical example of an entropy-driven process. *J. Biol. Chem.* **262**(32), 15696–15701 (1987).

[45] Orgel, J. P. R. O., Irving, T. C., Miller, A., and Wess, T. J. Microfibrillar structure of type I collagen *in situ*. *Proc. Natl. Acad. Sci. USA* **103**, 9001–9005 (2006).

[46] Giraud-Guille, M. M., Mosser, G., and Belamie, E. Liquid crystallinity in collagen systems in vitro and in vivo. *Curr. Opin. Colloid In.* **13**(4), 303–313 (2008).

[47] Gobeaux, F., Mosser, G., Anglo, A., Panine, P., Davidson, P., Giraud-Guille, M. M., and Belamie, E. Fibrillogenesis in dense collagen solutions: a physicochemical study. *J. Mol. Biol.* **376**(5), 1509–1522 (2008).

[48] Kirkwood, J. E. and Fuller, G. G. Liquid crystalline collagen: a self-assembled morphology for the orientation of mammalian cells. *Langmuir* **25**(5), 3200–3206 (2009).

[49] Balzer, F., Kankate, L., Niehus, H., and Rubahn, H. G. Epitaxy vs. dipole

assisted growth for organic oligomer nanoaggregates. *Proc. SPIE* **5925**, 59250A (2005).

[50] Stachel, I., Schwarzenbolz, U., Henle, T., and Meyer, M. Cross-linking of type I collagen with microbial transglutaminase: Identification of cross-linking sites. *Biomacromolecules* **11**(3), 698–705 (2010).

[51] Sun, M., Stetco, A., and Merschrod S., E. F. Surface-templated formation of protein microfibril arrays. *Langmuir* **24**(10), 5418–5421 (2008).

[52] Schlegel, M. L., Nagy, K. L., Fenter, P., Cheng, L., Sturchio, N. C., and Jacobsen, S. D. Cation sorption on the muscovite (001) surface in chloride solutions using high-resolution X-ray reflectivity. *Geochim. Cosmochim. Ac.* **70**(14), 3549–3565 (2006).

[53] Müller, K. and Chang, C. C. Electric dipoles on clean mica surfaces. *Surf. Sci.* **14**(1), 39–51 (1969).

[54] Simbrunner, C., Nabok, D., Hernandez-Sosa, G., Oehzelt, M., Djuric, T., Resel, R., Romaner, L., Puschnig, P., Ambrosch-Draxl, C., Salzmann, I., Schwabegger, G., Watzinger, I., and Sitter, H. Epitaxy of rodlike organic molecules on sheet silicates – A growth model based on experiments and simulations. *J. Am. Chem. Soc.* **133**, 3056–3062 (2011).

[55] Maslova, M. V., Gerasimova, L. G., and Forsling, W. Surface properties of cleaved mica. *Colloid J.* **66**(3), 322–328 (2004).

[56] Heinz, H., Castelijns, H. J., and Suter, U. W. Structure and phase transitions of alkyl chains on mica. *J. Am. Chem. Soc.* **125**(31), 9500–9510 (2003).

[57] Mertz, E. L. and Leikin, S. Interactions of inorganic phosphate and sulfate anions with collagen. *Biochemistry* **43**(47), 14901–14912 (2004).

[58] Balzer, F. and Rubahn, H. G. Dipole-assisted self-assembly of light-emitting p-nP needles on mica. *Appl. Phys. Lett.* **79**(23), 3860–3862 (2001).

[59] Karsai, Á., Grama, L., Murvai, Ü., Soós, K., Penke, B., and Kellermayer, M. S. Z. Potassium-dependent oriented growth of amyloid β25–35 fibrils on mica. *Nanotechnology* **18**, 345102 (2007).

[60] Karsai, Á., Murvai, Ü., Soós, K., Penke, B., and Kellermayer, M. S. Oriented epitaxial growth of amyloid fibrils of the n27c mutant β25–35 peptide. *Eur. Biophys. J.* **37**(7), 1133–1137 (2008).

[61] Nelson, R. and Eisenberg, D. Recent atomic models of amyloid fibril structure. *Curr. Opin. Struct. Biol.* **16**(2), 260–265 (2006).

[62] Jiang, H. and Grinnell, F. Cell–matrix entanglement and mechanical anchorage of fibroblasts in three-dimensional collagen matrices. *Mol. Biol. Cell* **16**(11), 5070–5076 (2005).

[63] Adams, J. C. Regulation of protrusive and contractile cell-matrix contacts. *J. Cell Sci.* **115**(2), 257–265 (2002).

[64] Li, R., Mitra, N., Gratkowski, H., Vilaire, G., Litvinov, R., Nagasami, C., Weisel, J., Lear, J., DeGrado, W., and Bennett, J. Activation of integrin α2bß3 by modulation of transmembrane helix associations. *Science* **300**(5620), 795 (2003).

APPENDIX A

FIGURES

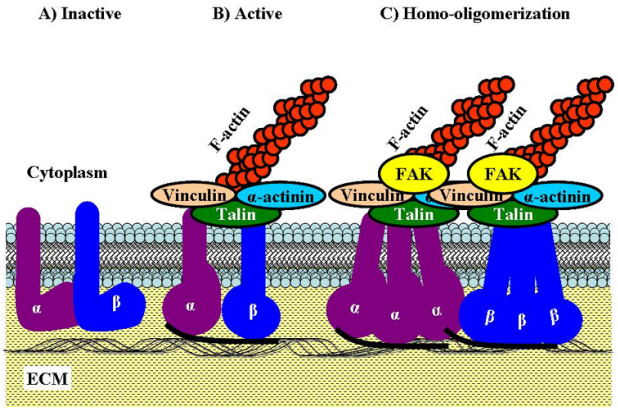

Fig. 1. Schematic view of the integrin at (A) inactive, (B) active and (C) homo-oligomerization state. (A) In inactive state, integrins do not bind to ligands and do not transduce signals. (B) Activation of integrin increases its affinity to the ligand, the ECM, (C) while clustering the α- and β-transmembrane domains forms homo-oligomer which increases the avidity of the complexes, aiding the formation of a focal adhesion. F-actin: Filamentous actin (Figure obtained from Ref. 64).

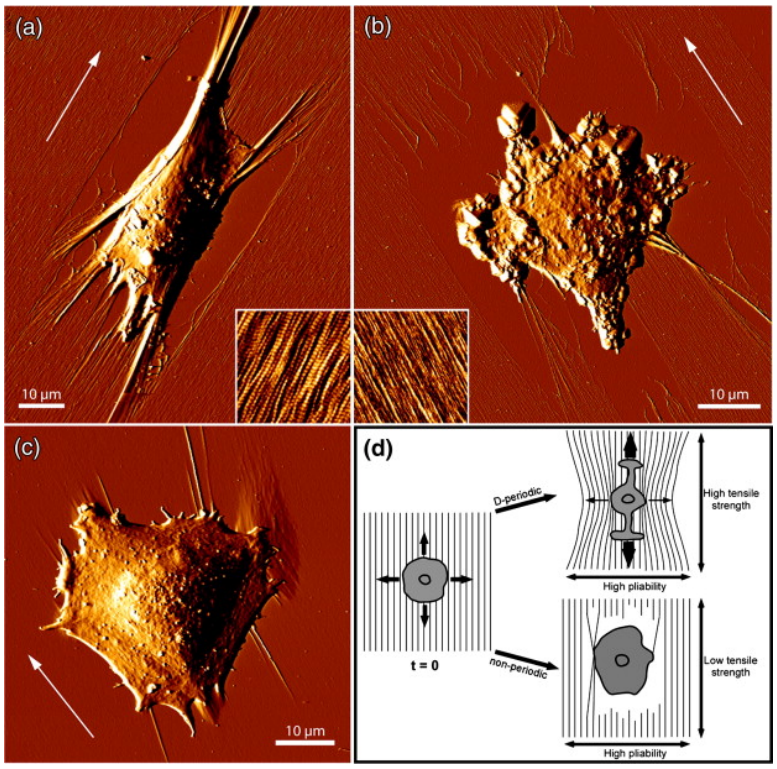

Fig. 2. AFM images of SAOS cell (Figure 2 from Ref. 21)[1] seeded on 2D aligned collagen layers. (a) Cell seeded on aligned collagen layers with D-period, showing cell polarization. (b) Cell seeded on non-periodic collagen layers, rupture of collagen fibrils observed and cell did not polarize. (c) Cell on cross-linked collagen layers showing neither cell polarization nor collagen deformation. (d) Model illustrating differences in matrix rigidity between D-periodic and non-periodic matrices affect cell polarization.

[1]Part of the data reported is reprinted from Friedrichs, J., Taubenberger, A., Franz, C. M., and Müller, D. J. Cellular remodelling of individual collagen fibrils visualized by time-lapse AFM. *J. Mol. Biol.* **372**(3), 594–607 (2007). Copyright (2007), with permission from Elsevier.

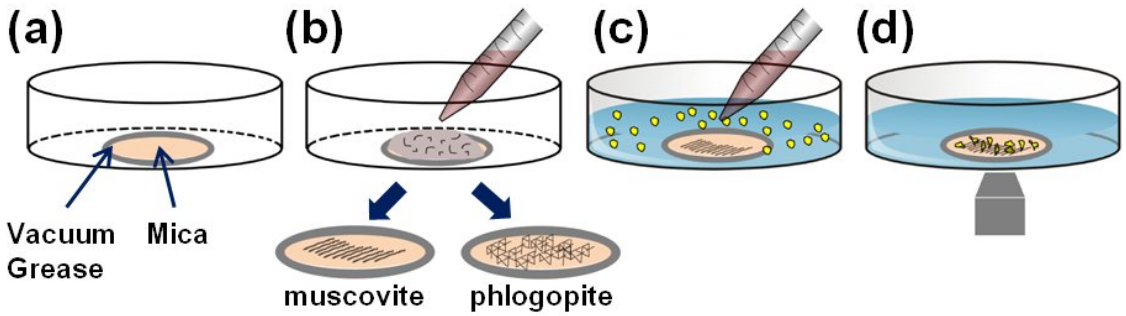

Fig. 3. Overview of the materials and methods. (a) Fresh cleaved mica was affixed to the glass bottom petri dish using vacuum grease around the mica edges contacting the petri dish. (b) Collagen-buffer solution was deposited onto the mica and incubated at room temperature overnight. On muscovite mica, collagen assembled into parallel fibrils; on phlogopite, triangular network. (c) Cells were seeded onto the collagen layers, incubated overnight at 37°C. (d) Cells were fixed and observed using Fluorescence Microscopy and AFM.

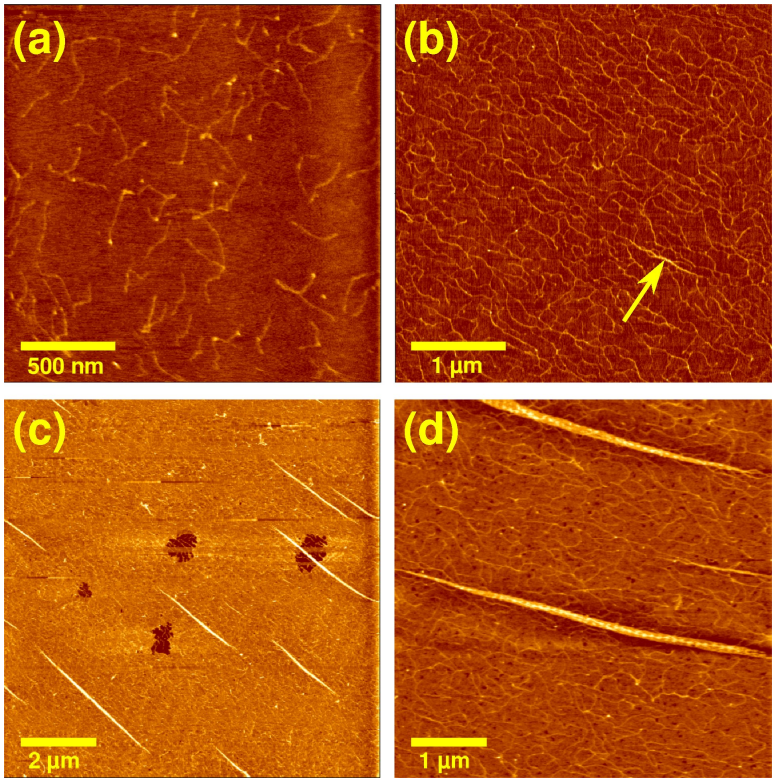

Fig. 4. Early stages of collagen assembly on muscovite[26]. 0.5 μg/ml collagen with 200 mM KCl. (a) 1-min incubation, showing randomly adsorbed collagen monomers. (b) 18-min incubation. A nascent fibril is marked by an arrow. (c,d) 30-min incubation, showing emergence of fibrils aligned in parallel. D-period is visible in (d).

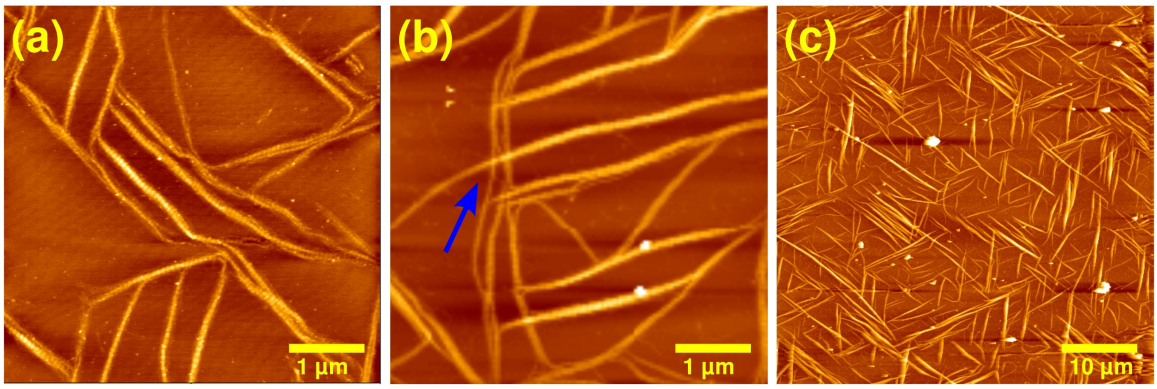

Fig. 5. AFM topography of triangular collagen networks on phlogopite, comparing the effects of glycine. Collagen concentration was 10 μg/ml for (a) and (b), and 30 μg/ml in (c). Incubated overnight. (a) Without glycine. (b) Glycine added to the sample, blue arrow denotes fibril crawling over the others instead of bending as with the case without glycine in (a). (c) Collagens with glycine cross-linked with mTG.

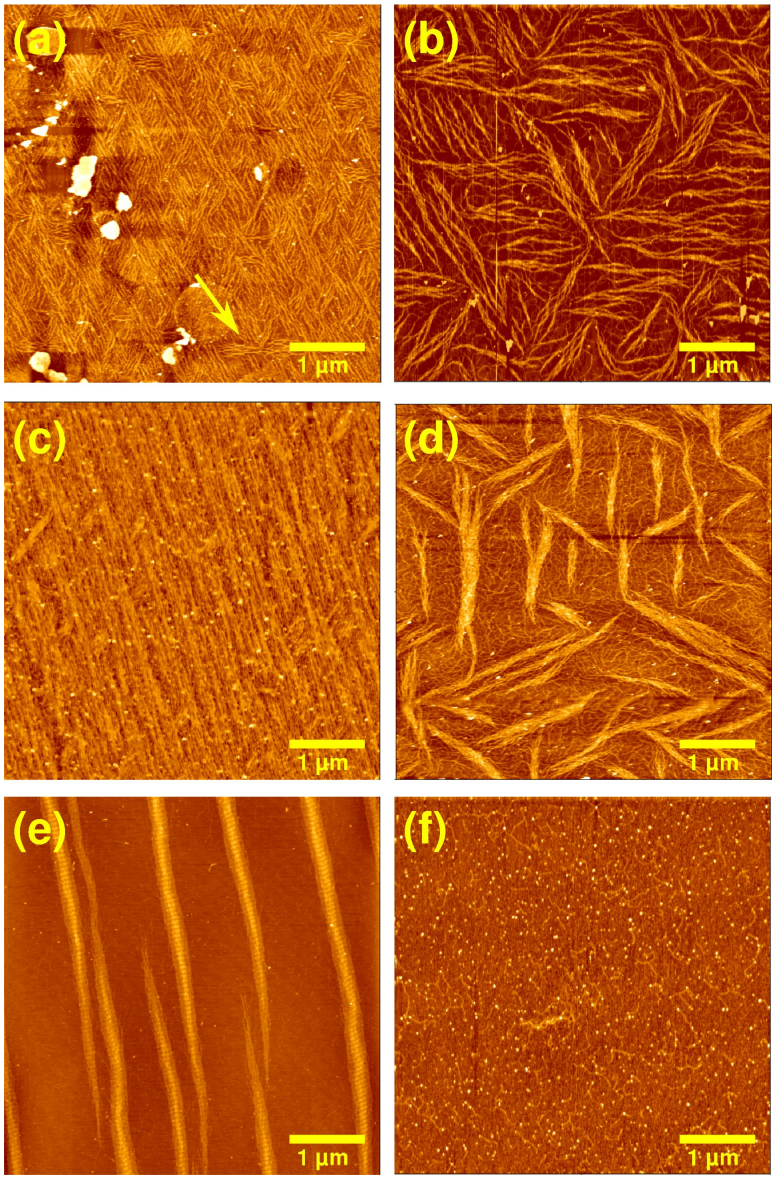

Fig. 6. Effect of K^+ on collagen assembly[26]. (a,c,e) Muscovite, (b,d,f) Phlogopite. All images are with 5 μg/ml collagen and 30-min incubation time. (a,b) 50 mM KCl. (a) Checkerboard-like, (b) triangular patterns. Arrow in (a) marks collagen fibrils aligned in a third direction. (c,d) 100 mM KCl. (c) Mostly unidirectional alignment, (d) bundling of collagen fibrils in the triangular pattern. (e,f) 400 mM KCl (e) Growth of parallel, thicker fibrils with D-periods, (f) no extensive assembly on phlogopite mica, suggesting weak adsorption.

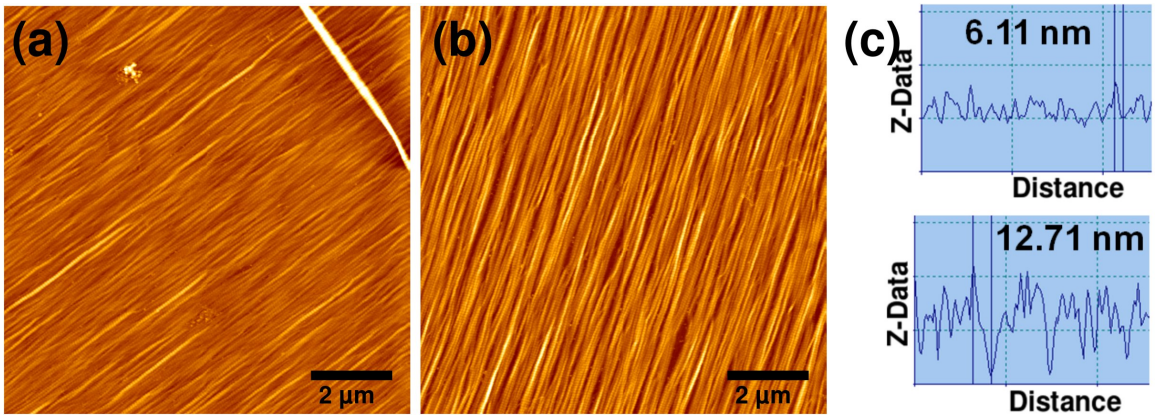

Fig. 7. AFM topography of aligned collagen fibrils on muscovite mica, comparing the effects of glycine. Collagen concentration at 30 μg/ml, incubated overnight. (a) Without glycine. (b) With glycine. (c) The height profiles of the fibrils without glycine (top) and with glycine (below).

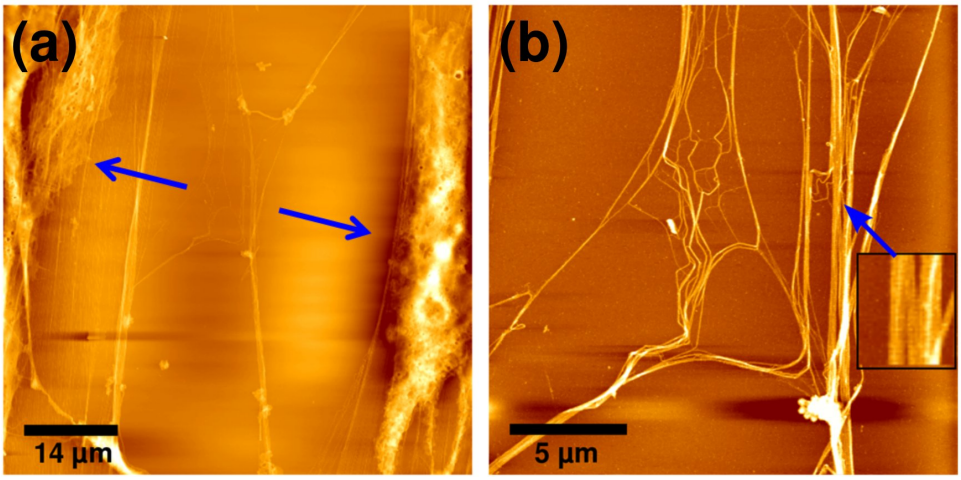

Fig. 8. AFM topography of collagens and cells on muscovite mica after 20 hours of cell seeding. Sample was fixed and dried. (a) Two cells pulling the anisotropic collagen fibrils resulting in matrix deformation. Blue arrow indicates cell pulling direction. (b) Zoom-in scan of the deformed fibrils, where inset shows presence of D-periods along the fibril.

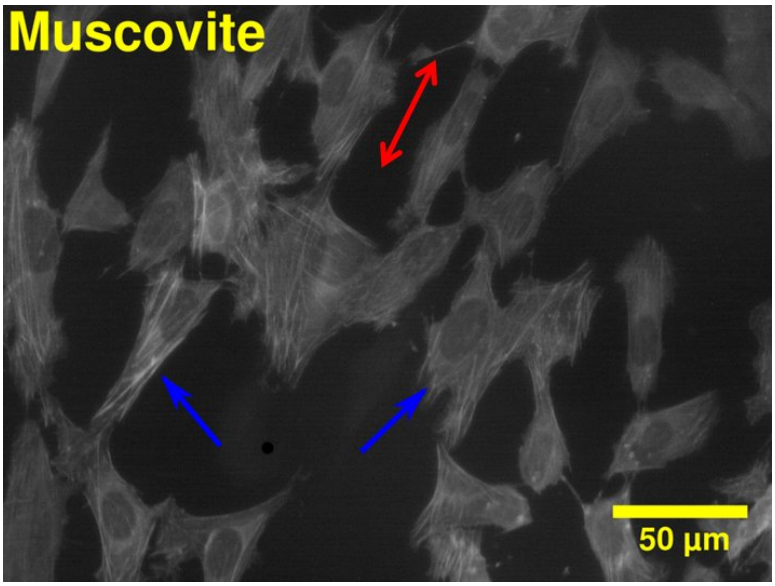

Fig. 9. Fluorescence image of U2OS cells on non-cross-linked aligned collagens on muscovite, taken 22.5 hours after cell seeding. Sample was fixed. Blue arrow indicates presence of stress fiber. Red double-ended arrow indicates overall cell polarization direction.

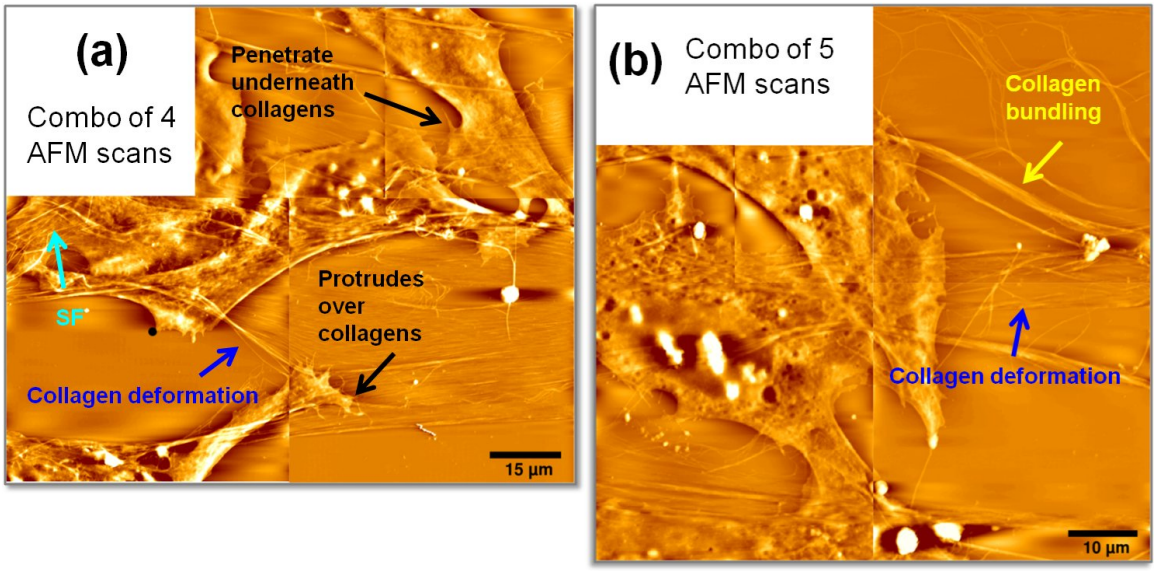

Fig. 10. Combination of AFM topography scans of collagens and cells on muscovite mica after 22.5 hours of cell seeding. Sample was fixed and dried. (a) Collagen deformation was apparent as cells reached out and pull (blue arrow). Part of some cells could penetrate underneath the collagen layers (black arrow). Stress fiber-like structures were observed (light blue arrow). (b) Collagen bundling was observed as cells deform the matrix (yellow arrow).

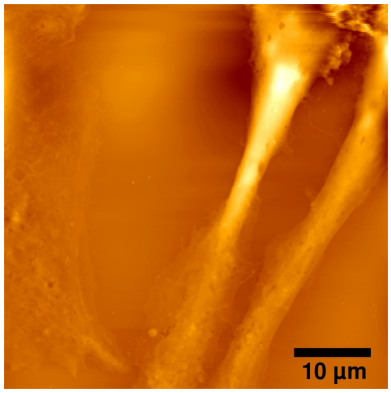

Fig. 11. AFM topography of collagens and cells on non-cross-linked collagens on phlogopite mica after 22 hours of cell seeding. Sample was fixed and dried. No collagens were observed.

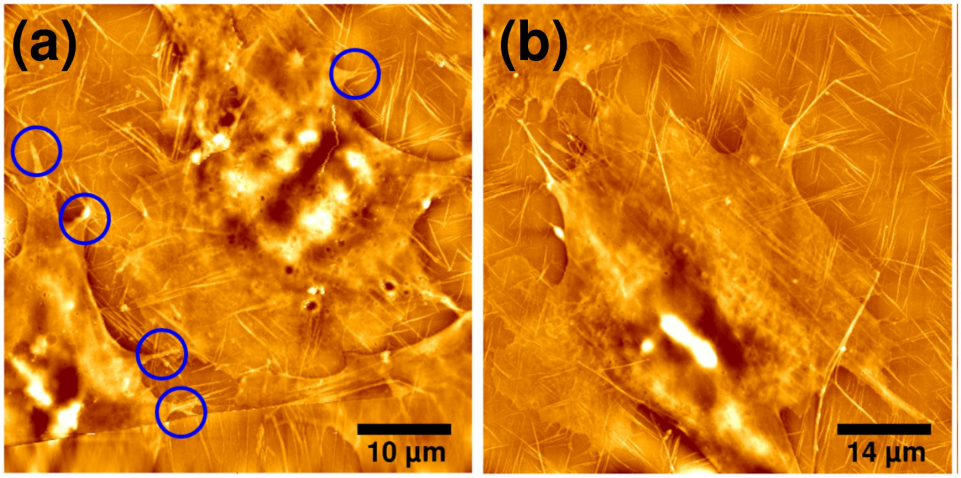

Fig. 12. AFM topography of collagens and cells on cross-linked collagens on phlogopite mica after 23 hours of cell seeding. Sample was fixed and dried. No apparent matrix deformation were observed. (a) Blue circlea indicate cells formed protrusions along the fibril directions. (b) A larger scan. Cells appeared rounder compared to the case of muscovite mica.

VITA

Name: Wee Wen Leow

Address: Department of Biomedical Engineering

5045 ETB

MS 3120 TAMU

College Station, TX 77843.

Email address: weewenleow@gmail.com

Education: B.S., Biomedical Engineering, Texas A&M University, 2009

M.S., Biomedical Engineering, Texas A&M University, 2012

The typist for this thesis was Wee Wen Leow.